Sliding Interleaved Cylinder (SLINCY) Imaging with Dynamic Center Frequency Adjustment

Kie Tae Kwon[1], Adam B. Kerr[1], Bob S. Hu[2,3], and Dwight G. Nishimura[1]

[1]*Electrical Engineering, Stanford University, Stanford, CA, United States,* [2]*Palo Alto Medical Foundation, Palo Alto, CA, United States,* [3]*HeartVista Inc., Los Altos, CA, United States*

Purpose: A sliding interleaved cylinder (SLINCY) acquisition is a variation of a sliding interleaved k_y (SLINKY) [1] acquisition where a 3D concentric cylinders trajectory [2] is employed instead of a 3DFT sequence. Compared to SLINKY, SLINCY offers faster scan times and more distributed artifacts from k-space amplitude modulation while equally suppressing venetian blind artifacts. Previously, we employed the SLINCY acquisition for a non-contrast-enhanced (NCE) magnetization-prepared 3D SSFP sequence to improve artery-vein contrast in the lower extremities [3]. However, one challenge for this approach is to cover a large FOV (> 30 cm) without SSFP banding artifacts to yield a uniform arterial signal. In this work, we exploited the thin-slab-scan nature of SLINCY to dynamically adjust the center frequency (CF) of each slab for banding artifact reduction using a separately acquired 2D field map [4].

Methods: SLINCY: The SLINCY acquisition consists of a series of overlapped thin slabs for volumetric coverage. For each thin slab, one of N interleaved subset of 3D concentric cylinders (Fig. 1a) is collected and the slab location is incremented by a distance equal to the resolution in the slab direction (Fig. 1b). After gridding, each slice is reconstructed by combining partial k-space data from a corresponding set of N consecutive slabs in a hybrid space (z-k_x-k_y). With a linear-phase RF pulse applied, k-space phase modulation is negligible across those N slabs. For the NCE magnetization-prepared 3D SSFP sequence for peripheral angiography, slabs are in the S/I direction and cylinders are collected in a centric-ordered and segmented way to capture the transient contrast from venous and fat saturation modules.

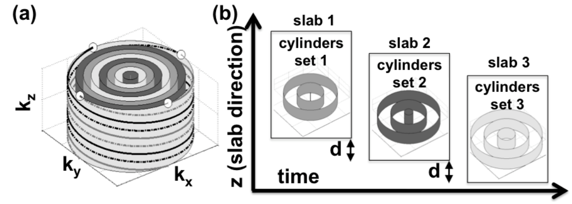

Fig. 1. (a) A 3D concentric cylinders k-space trajectory depicted with nine cylinders. Four helical readouts are shown on the outermost cylinder. **(b)** Data acquisition scheme of SLINCY. A subset of the cylinders is collected at each slab in an interleaved way (N = 3), incremented by a distance d equal to the resolution in z between slabs.

Dynamic CF adjustment: Considering the relatively long TR (6~8 ms) typically used in SLINCY, SSFP banding artifacts can be non-negligible for the application of peripheral angiography, where significant z^2 field variation may exist in the S/I direction. To address this issue, a 2D coronal field map was briefly acquired prior to the scan, targeting the deep arteries of interest whose range is limited in the A/P direction and more directional in the S/I direction. With the field map, the CF of each thin slab of SLINCY can be adjusted to reflect the average off-resonance frequency of its mid-slice (Fig. 2b). If each slab is thin enough to lie in the passband of the SSFP frequency profile centered at its CF, slices can be reconstructed with minimal k-space amplitude modulation from the variations across the passband of the profile (Fig. 2a). In addition, this scheme can mitigate the misalignment of the location of each slab by adding its off-resonance frequency to the frequency associated with the slab-selective gradient for off-isocenter imaging in the slab direction.

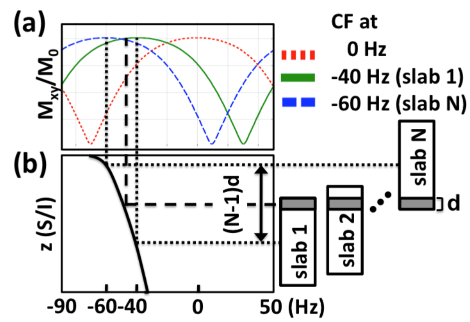

Fig. 2. (a) SSFP frequency profile (TE/TR = 3.5/7.0 ms, flip angle = 70°) of arterial blood (T1/T2 = 1273/254 ms at 1.5 T) centered at different CFs. **(b)** Dynamic CF adjustment scheme for SLINCY using a 2D field map averaged in the R/L direction. The CF of each slab is adjusted with the average off-resonance frequency of its mid-slice. With a thin slab, each slice (gray element) can lie in the pass-bands of N consecutive slabs (-60 ~ -40 Hz).

Imaging Parameters: In vivo studies of the lower extremities on healthy volunteers were performed on a GE Excite 1.5 T scanner with an 8-channel cardiac coil. The 2D coronal field map was acquired from an SPGR sequence with isotropic resolution = 2 mm, FOV = 340×340 mm^2, slice thickness = 10 mm, and TEs = 4.6, 9.2 ms. Gradients for the SSFP version of the SLINCY acquisition were designed to provide isotropic resolution = 1.2 mm and FOV = 340×340×28.8 mm^3 for each slab. TE/TR = 3.5/7.0 ms, and flip angle = 70°. A total of 275 slabs were acquired to cover 31 cm in the S/I direction. Total scan time was 6 minutes. Images were reconstructed with 3D gridding followed by a SLINCY reconstruction (N = 16) and a maximum-intensity-projection (MIP) with a factor of two zero-padding in all dimensions.

Results: Figure 3 demonstrates that the dynamic CF adjustment scheme for SLINCY is feasible without any observable artifacts from k-space amplitude modulation. This scheme successfully reduces the banding artifacts (Fig. 3c), which otherwise degrade the depiction of arterial signal in the lower extremities (Fig. 3b). Noticeable improvements are observed near -70 Hz (≈ -1/(2TR)) around the edge in the S/I direction (Fig. 3a).

Discussion and Conclusion: We demonstrated the feasibility of the dynamic CF adjustment scheme for SLINCY that improves the uniformity of arterial signal using a separately acquired 2D field map. The extra time for acquiring and post-processing the field map is much less than that of acquiring multiple phase-cycled datasets for banding artifact reduction. Because SLINCY distributes artifacts from k-space amplitude modulation over the x-y plane, employing a longer TR with a narrower SSFP passband can still be feasible for faster scan times. In the future, we will also explore dynamic shimming [5] to improve the robustness of this approach.

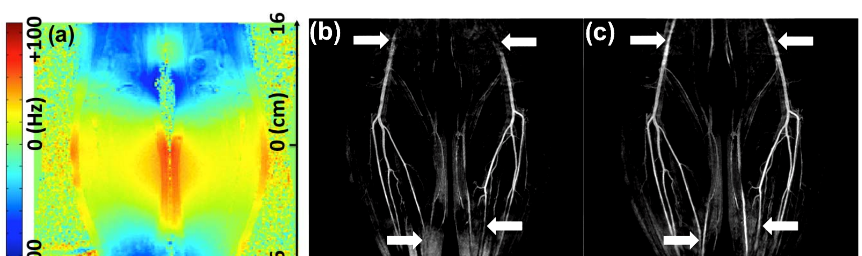

Fig. 3. Coronal images of the calf of a normal volunteer: **(a)** Field map **(b)** MIP image with regular SLINCY **(c)** MIP image with dynamic CF adjustment for SLINCY. Solid arrows show the reduction of banding artifacts in (c) compared to (b).

References: [1] Liu et al., JMRI 1998;8:903.
[2] Ruppert et al., 11th ISMRM, p.208, 2003.
[3] Kwon et al., 20th ISMRM, p.3898, 2012.
[4] Graves et al., JMRI 2009;29:1230.
[5] Morrell et al., MRM 1997;38:477.